ECOLOGY

Large losses of ammonium-nitrogen from a rice ecosystem under elevated CO_2

Chenchao Xu[1], Kaihang Zhang[1], Wanying Zhu[1], Jing Xiao[1], Chen Zhu[1], Naifang Zhang[1], Fangjian Yu[1], Shuyao Li[1], Chunwu Zhu[2], Qichao Tu[3], Xin Chen[1], Jianguo Zhu[2], Shuijin Hu[4], Roger T. Koide[5], Mary K. Firestone[6], Lei Cheng[1]*

Inputs of nitrogen into terrestrial ecosystems, mainly via the use of ammonium-based fertilizers in agroecosystems, are enormous, but the fate of this nitrogen under elevated atmospheric carbon dioxide (CO_2) is not well understood. We have taken advantage of a 15-year free-air CO_2 enrichment study to investigate the influence of elevated CO_2 on the transformation of ammonium-nitrogen in a rice ecosystem in which ammonium is usually assumed to be stable under anaerobic conditions. We demonstrate that elevated CO_2 causes substantial losses of ammonium-nitrogen that result from anaerobic oxidation of ammonium coupled to reduction of iron. We identify a new autotrophic member of the bacterial order Burkholderiales that may use soil CO_2 as a carbon source to couple anaerobic ammonium oxidation and iron reduction. These findings offer insight into the coupled cycles of nitrogen and iron in terrestrial ecosystems and raise questions about the loss of ammonium-nitrogen from arable soils under future climate-change scenarios.

INTRODUCTION

Increased plant biomass accumulation in response to elevated atmospheric CO_2 (eCO_2) is largely constrained by limited soil nitrogen (N) availability (*1*–*7*), so increasing the supply of N is expected to mitigate CO_2 emissions and associated climate warming by sustaining the CO_2 enhancement of carbon (C) storage in terrestrial ecosystems (*1*–*7*). Ecosystem inputs of human-made N compounds, mostly in the form of ammonium (NH_4^+)–based fertilizers, are enormous, but the distribution between natural and managed/agricultural systems is unbalanced (*8*–*12*). The majority of NH_4^+ fertilizers have been applied to agroecosystems (*8*–*14*), driven by a growing global demand for food. In particular, the global application of NH_4^+ fertilizers to rice ecosystems, which supply the staple food to more than half of the world's population, was estimated at 19 Tg N in 2015, ~20% of N fertilizer use in all crops (*8*), and this value is projected to increase under future eCO_2 (*8*–*11*). Increasing the use of NH_4^+ over nitrate (NO_3^-) fertilizers may enhance the growth of rice plants under eCO_2, in part because plants under eCO_2 prefer NH_4^+ over NO_3^- (*5*, *6*). However, whether high NH_4^+ inputs sustain the response of rice ecosystems to eCO_2 hinges, in part, on the extent to which eCO_2 influences the stability of NH_4^+ in paddy soils, especially under anaerobic conditions.

RESULTS AND DISCUSSION

Effects of eCO_2 and N supply on plant N uptake

Here, we present results from a long-term free-air CO_2 enrichment (FACE) study in which three ambient (aCO_2) and three elevated (ambient + 200 μmol mol^{-1} CO_2) atmospheric CO_2 plots have been maintained to investigate the response of a rice ecosystem to eCO_2 (fig. S1) (*15*, *16*). We first examined the effect of eCO_2 on rice growth at seven levels of NH_4^+ fertilization: 0, 8, 12.5, 15, 22.5, 25, and 35 g urea-N m^{-2} (see Materials and Methods). At each N level, eCO_2 significantly increased aboveground biomass of rice plants ($P < 0.01$; fig. S2A). Theory predicts (*1*, *3*, *4*) that the net CO_2 effect on plant N uptake should be higher with high N supply than with low N supply, regardless of whether it is within a N-limited or a N-rich system (fig. S2B). However, eCO_2 did not increase plant N uptake as much as anticipated at high N supply compared to low N supply both across the four rice growth stages in an early experimental year (fig. S2C) and for the entire experimental period (fig. S2D). The CO_2-induced aboveground alterations such as photosynthetic acclimation (*17*) and tissue N concentrations (fig. S2A) could not adequately explain the lower than expected net CO_2 effect on plant N uptake, especially at high compared to low levels of NH_4^+-N supply (fig. S2, C and D). We, therefore, reason that alterations in NH_4^+-N transformation in the soil may contribute partly to the CO_2-induced negative feedback on plant N uptake in the rice paddy system.

N loss via AOA under eCO_2

We explored the possible microbial mechanisms by which eCO_2 transforms NH_4^+-N in the paddy soil. We first used metagenomic sequencing to analyze microbial functional genes associated with N cycling in the field (see Materials and Methods). Compared to aCO_2, eCO_2 increased the abundance of many functional genes, especially those involved in anaerobic N transformations (fig. S3). For much of the time rice is growing, anaerobic conditions prevail in paddy soils. In previous work, we demonstrated that eCO_2 promoted soil anaerobic conditions by stimulating microbial activity and decreasing redox potential in the rice paddy system (*15*). In this research, we further investigated the CO_2 effect on the NH_4^+-N transformations under anaerobic conditions by conducting three separate but complementary experiments (see Materials and Methods). Experiment 1 included two parallel microcosm experiments carried out in 2014 and 2015 (Fig. 1A). Experiment 2 was an in situ field

[1]MOE Key Laboratory of Biosystems Homeostasis & Protection, College of Life Sciences, Zhejiang University, Hangzhou 310058, China. [2]State Key Laboratory of Soil and Sustainable Agriculture, Institute of Soil Science, Chinese Academy of Sciences, Nanjing 210008, China. [3]Institute of Marine Science and Technology, Shandong University, Jinan 250100, China. [4]Department of Plant Pathology, North Carolina State University, Raleigh, NC 27695, USA. [5]Department of Biology, Brigham Young University, Provo, UT 84602, USA. [6]Department of Environmental Science, Policy and Management, University of California, Berkeley, Berkeley, CA 94720, USA.
*Corresponding author. Email: lcheng@zju.edu.cn

study conducted in 2016 (Fig. 1B). Experiment 3 consisted of two parallel stable isotope probing (SIP) microcosm experiments performed in 2017 (Fig. 1C). We determined whether NH_4^+-N could be converted to an oxidized form using ^{15}N-NH_4^+ in experiments 1 and 2. We measured the rate of NH_4^+ consumption in experiment 3.

We found that eCO_2 led to considerable losses of N from the anaerobic paddy soil when NH_4^+ was added alone (hereafter $+NH_4^+$) in experiments 1 to 3. In experiment 1 in which soils were amended with $^{15}NH_4^+$ (Fig. 1A), headspace ^{15}N-labeled N_2 ($^{30}N_2 + {}^{29}N_2$) production averaged across two experimental years was significantly higher in eCO_2 (3.84 ± 0.08 μg N g^{-1} day^{-1}) than in aCO_2 soils (3.45 ± 0.13 μg N g^{-1} day^{-1}; $P < 0.05$; Fig. 1D). The magnitude of the CO_2 effect on ^{15}N-N_2 production following $^{15}NH_4^+$ addition was even larger in the field (Fig. 1B); in situ ^{15}N-N_2 production under eCO_2 (44.37 ± 2.06 mg N m^{-2} day^{-1}) was 88% higher than that under aCO_2 ($P < 0.01$; Fig. 1D). In experiment 3 (Fig. 1C), similarly, the average rate of NH_4^+ consumption increased significantly with eCO_2 (3.61 ± 0.42 μg N g^{-1} day^{-1}) compared to aCO_2 (2.61 ± 0.43 μg N g^{-1} day^{-1}) across the two SIP microcosms ($P < 0.05$; Fig. 1D). These results suggest that the eCO_2-associated NH_4^+-N loss was a consequence of anaerobic oxidation of ammonium (AOA) in the paddy soil.

AOA coupled to IR under eCO_2

Soils contain a variety of compounds capable of catalyzing oxidation reactions under anaerobic conditions, and iron oxides are among the most abundant (see Discussions I and II in the Supplementary Materials) (*15*, *18*, *19*). In the rice-FACE system, we previously demonstrated that eCO_2 significantly stimulated root and microbial respiration, decreased soil redox potential, and facilitated ferric iron reduction (IR) (*15*). To test whether eCO_2-induced changes in IR were coupled to AOA, we investigated the CO_2 effect on ferrous iron (Fe^{2+}) production in soils with the addition of either amorphous ferric oxyhydroxide alone [hereafter $+Fe_{(III)}$] or NH_4^+ and $Fe_{(III)}$ together [hereafter $+NH_4^+ + Fe_{(III)}$] in experiment 1 (fig. S4A). Both the $+NH_4^+ + Fe_{(III)}$ and $+Fe_{(III)}$ treatments enhanced Fe^{2+} production, with the average rate of the former being 1.7-fold faster than that of the latter across two experimental years ($P < 0.01$; fig. S5, A and B). The stimulatory effect of $+NH_4^+$ on Fe^{2+} production [$+NH_4^+ + Fe_{(III)}$ versus $+Fe_{(III)}$] was further reinforced by eCO_2 (64%) compared to aCO_2 (41%; Fig. 2B and fig. S5, A and B).

We then compared the CO_2 effect on ^{15}N-N_2 production when soils were given either $+{}^{15}NH_4^+ + Fe_{(III)}$ or $+{}^{15}NH_4^+$ in experiment 1. The $+{}^{15}NH_4^+ + Fe_{(III)}$ treatment produced ^{15}N-N_2 2.4-fold faster

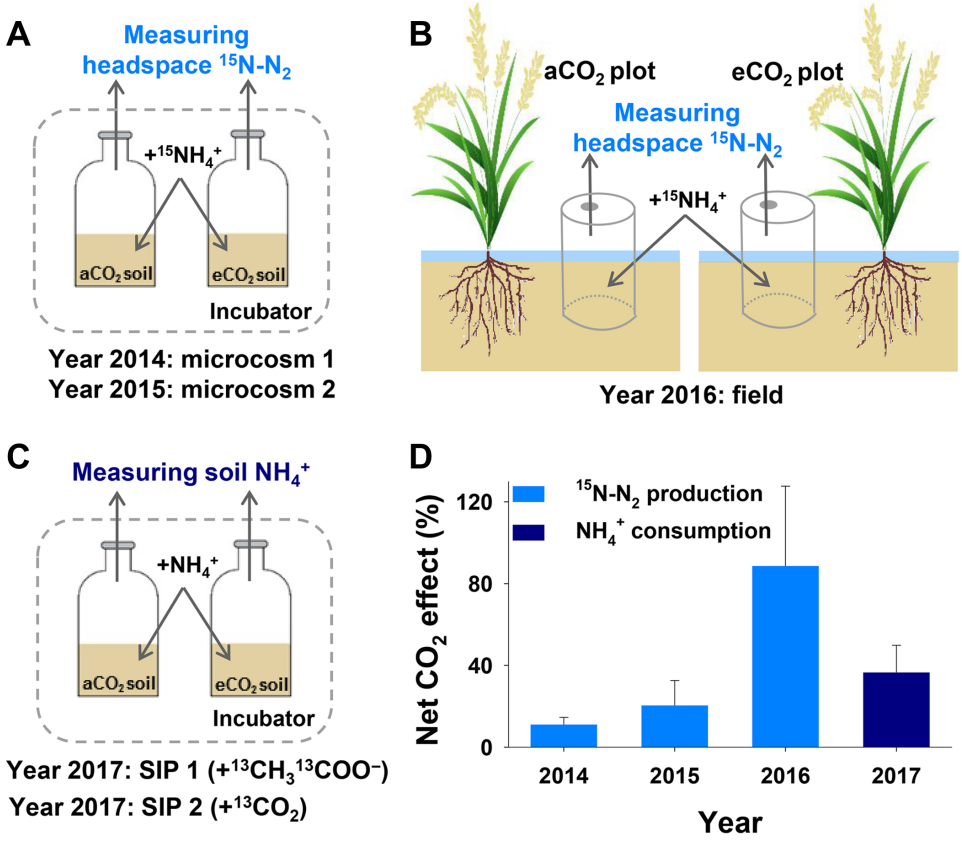

Fig. 1. Losses of ammonium (NH_4^+)–nitrogen from a rice ecosystem exposed to long-term FACE. (**A** to **C**) Experimental scheme: experiment 1 (A), two parallel microcosms in which soils, taken from ambient (aCO_2) and elevated (eCO_2) CO_2 plots at the heading stage of rice plants in 2014 and 2015, were incubated with the addition of $^{15}NH_4^+$ under strictly anaerobic conditions; experiment 2 (B), a field work with an anaerobic bioreactor conducted in the 2016 rice growing season; experiment 3 (C), two parallel SIP microcosms in which soils, taken from aCO_2 and eCO_2 plots in the 2017 rice growing season, were anaerobically incubated with the addition of ^{13}C-labeled either $^{13}CH_3{}^{13}COO^- + NH_4^+$ (SIP 1) or $^{13}CO_2 + NH_4^+$ (SIP 2). (**D**) Influence of eCO_2 on ^{15}N-N_2 production (total amount of $^{29}N_2$ and $^{30}N_2$; light blue bars) in experiments 1 ($P < 0.05$) and 2 ($P < 0.01$), and NH_4^+ consumption (dark blue bar) in experiment 3 ($P < 0.05$). The net CO_2 effect was calculated: (value at eCO_2 − value at aCO_2)/(value at aCO_2). Values are means ($n = 3$) ± SEM.

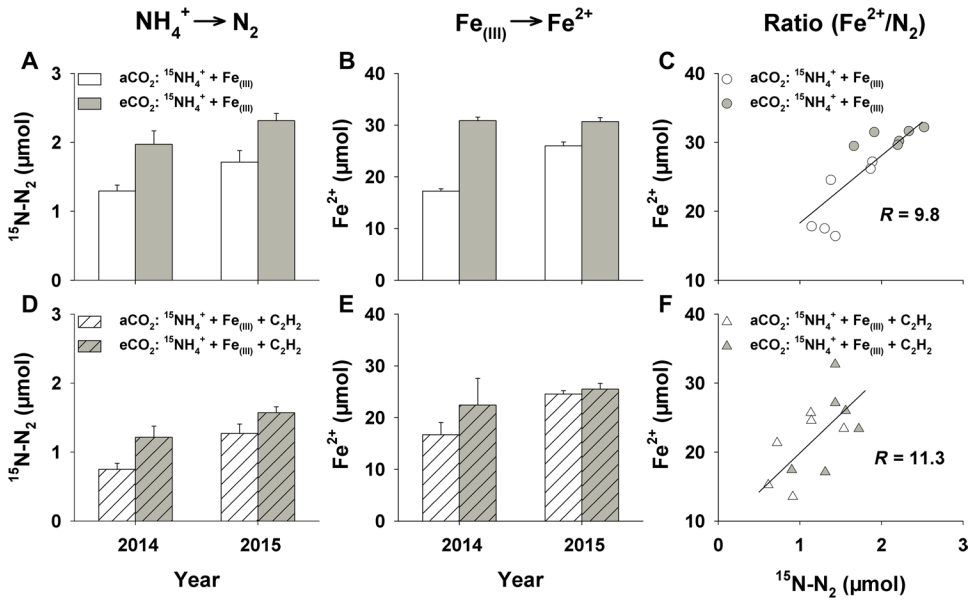

Fig. 2. AOA coupled to IR under elevated CO_2. Elevated CO_2 increased the production of ^{15}N-N_2 (total amount of $^{29}N_2$ and $^{30}N_2$) (**A** and **D**) and Fe^{2+} (**B** and **E**) following the addition of $^{15}NH_4^+ + Fe_{(III)}$ (A and B) or $^{15}NH_4^+ + Fe_{(III)} + C_2H_2$ together (D and E) in experiment 1 (see fig. S4A for the experimental scheme). (A and D) AOA ($NH_4^+ \rightarrow N_2$); CO_2 effect: $P < 0.01$; C_2H_2 effect: $P < 0.05$. (B and E) IR [$Fe_{(III)} \rightarrow Fe^{2+}$]; CO_2 effect: $P < 0.05$; C_2H_2 effect: $P = 0.61$. Open bars, ambient CO_2 (aCO_2); filled bars, elevated CO_2 (eCO_2). Data represent means ($n = 3$) ± SEM. (**C** and **F**) The stoichiometry of AOA-IR reactions and the overall molar ratio (R) of Fe^{2+} to ^{15}N-N_2, following the addition of either $+^{15}NH_4^+ + Fe_{(III)}$ (C) or $+^{15}NH_4^+ + Fe_{(III)} + C_2H_2$ (F), were estimated using a general linear model.

than did the $+^{15}NH_4^+$ treatment across two experimental years ($P < 0.01$; fig. S6, A and B). Corresponding to the CO_2 stimulation of N_2 production following $+^{15}NH_4^+$ (fig. S6, A and B), ^{15}N-N_2 production following $+^{15}NH_4^+ + Fe_{(III)}$ addition was increased, on average, by 40% in eCO_2 compared to aCO_2 soils ($P < 0.01$; Fig. 2A and fig. S6, A and B). These results indicate that the CO_2 enhancement of N_2 production was a result of AOA coupled to IR [AOA-IR; also referred to as Feammox (*19*)] in the paddy soil.

We also examined whether AOA-IR occurred in experiment 2 (fig. S4B). Again, relative to the $+NH_4^+$ treatment, the $+NH_4^+ + Fe_{(III)}$ treatment increased the production of Fe^{2+} ($P < 0.05$; fig. S5C) and ^{15}N-N_2 ($P < 0.05$; fig. S6C), confirming the occurrence of AOA-IR in the field. The CO_2 stimulation of AOA-IR was evidenced by the CO_2 enhancement of Fe^{2+} ($P < 0.05$; fig. S5C) and ^{15}N-N_2 ($P < 0.05$; fig. S6C) production in the $+NH_4^+ + Fe_{(III)}$ treatment. By mass balance (see Materials and Methods), we estimated that N_2 production throughout the rice growing season via AOA-IR following $+NH_4^+ + Fe_{(III)}$ accounted for 17 and 25% of the applied NH_4^+-N, respectively, under aCO_2 and eCO_2 plots.

Thermodynamically, three reactions of AOA-IR coupling are feasible in paddy soils (see Materials and Methods)

$$3Fe(OH)_3 + 5H^+ + NH_4^+ \rightarrow 3Fe^{2+} + 9H_2O + 0.5N_2 \quad (\Delta G^{\circ\prime} = -202\ kJ\ mol^{-1}) \quad (1)$$

$$6Fe(OH)_3 + 10H^+ + NH_4^+ \rightarrow 6Fe^{2+} + 16H_2O + NO_2^- \quad (\Delta G^{\circ\prime} = -79\ kJ\ mol^{-1}) \quad (2)$$

$$8Fe(OH)_3 + 14H^+ + NH_4^+ \rightarrow 8Fe^{2+} + 21H_2O + NO_3^- \quad (\Delta G^{\circ\prime} = -88\ kJ\ mol^{-1}) \quad (3)$$

where $\Delta G^{\circ\prime}$ is the energy yield of the redox reaction that was calculated at pH 6.5, as the pH value of most paddy soils under waterlogging is approximately neutral (*20*). Reaction 1 produces N_2, while reactions 2 and 3 yield NO_2^- and NO_3^-. Both NO_2^- and NO_3^- could be subsequently converted to N_2 through the reduction of NO_3^-/NO_2^- to N_2 (denitrification) (*9*) and/or AOA coupled to nitrite reduction (NR; AOA-NR, also referred to as anammox) (*21*, *22*). Two lines of evidence, however, suggest that AOA-NR contributes little to N_2 production in the rice-FACE system. First, $^{29}N_2$ production did not differ between the $+^{15}NH_4^+$ and $+^{15}NH_4^+ + {}^{14}NO_3^-$ treatment in AOA-NR tests accompanying with experiments 1 ($P = 0.44$; figs. S4A and S7A) and 2 ($P = 0.76$; figs. S4B and S7B). Second, the expression of *hzs*A, a gene encoding the subunit of hydrazine (N_2H_4) synthase in anammox bacteria (*22*), was not detectable in experiment 1 (table S1). If reactions 2 and 3 generated N_2 through denitrification, the addition of acetylene (C_2H_2), an inhibitor of the reduction of N_2O to N_2 during denitrification (*23*), would lower N_2 production. As expected, the presence of C_2H_2 reduced N_2 production, on average, by 34% ($P < 0.05$; Fig. 2, A and D, and fig. S6, A and B), whereas it did not alter Fe^{2+} production ($P = 0.61$; Fig. 2, B and E) following $+NH_4^+ + Fe_{(III)}$ addition across two experimental years.

To assess the relative contributions of the three reactions to N_2 production, we analyzed the stoichiometry of AOA-IR reactions in experiment 1. Because eCO_2 did not alter the Fe^{2+}:N_2 ratio either with ($P = 0.18$) or without ($P = 0.90$) C_2H_2, we used a general linear model to calculate the overall Fe^{2+}:N_2 ratio across two CO_2 treatments (see Materials and Methods). The Fe^{2+}:N_2 ratio was estimated to be 9.8:1 (Fig. 2C), suggesting that reaction 1 co-occurred with reaction 2 and/or reaction 3, as their theoretical mole ratios are 6:1, 12:1, and 16:1, respectively. The presence of C_2H_2 impeded denitrification and, as a result, increased the Fe^{2+}:N_2 ratio (Fig. 2F). Although we could not distinguish N_2 production from reactions 2

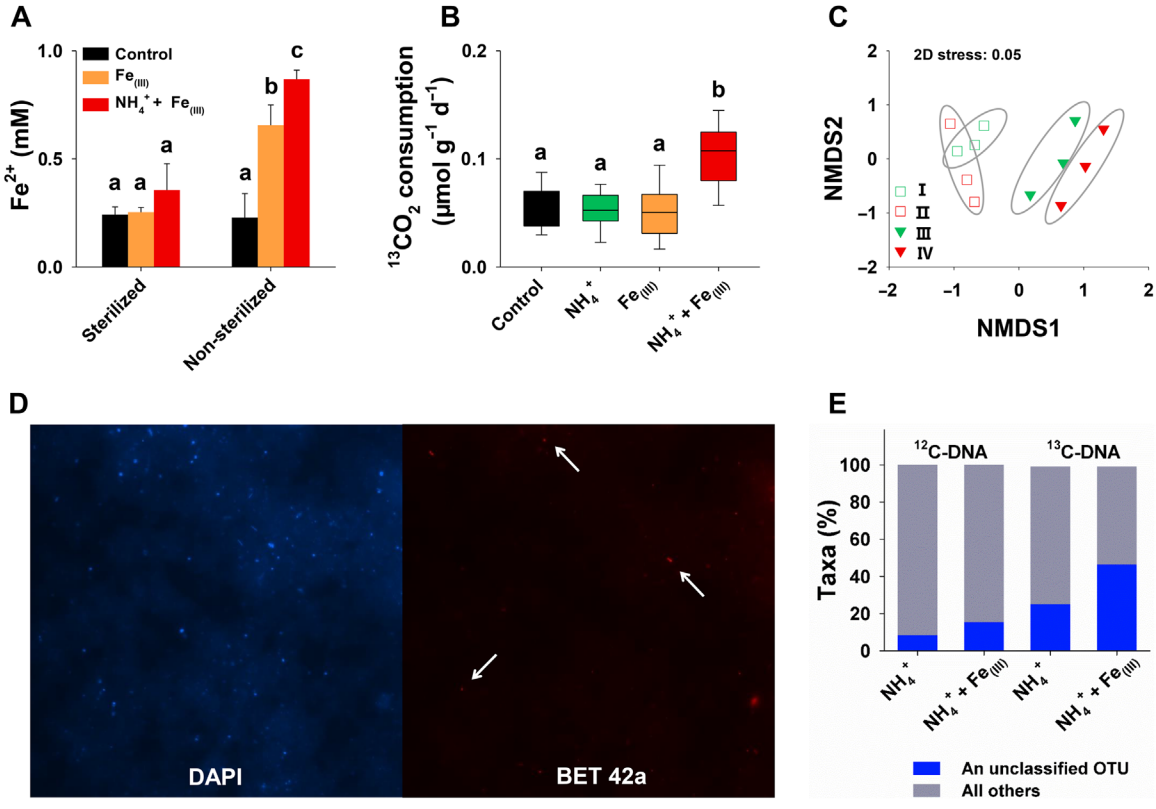

Fig. 3. Microbial mediation of the coupling of AOA and IR. (**A**) Fe^{2+} production following the addition of $Fe_{(III)}$ or NH_4^+ + $Fe_{(III)}$ after 2-week incubation using sterilized or nonsterilized soils. (**B**) $^{13}CO_2$ consumption following the addition of NH_4^+, $Fe_{(III)}$, or NH_4^++$Fe_{(III)}$ (experiment 3). Different letters above bars denote statistically significant differences ($P < 0.05$). (**C**) Nonmetric multidimensional analysis (NMDS) of community dissimilarities based on 16*S* rRNA gene profiling in experiment 3 (see fig. S4C for the experimental scheme). Squares (I and II), ^{12}C-DNA; triangles (III and IV), ^{13}C-DNA; green symbols (I and III), +NH_4^+; red symbols (II and IV), +NH_4^+ + $Fe_{(III)}$. (**D**) Images of live members of β-Proteobacteria using FISH during incubation (experiment 3). DAPI, 4′,6-diamidino-2-phenylindole (blue). The BET 42a probe (red) was used to target β-Proteobacteria. (**E**) Unclassified OTU dominated in both ^{12}C- and ^{13}C-labeled microbiota (experiment 3). Data are the relative abundance of taxa.

and 3, the proportion of N_2 produced from reaction 1 was estimated to account for 76% of the total N_2 production in experiment 1 (see Materials and Methods).

Microbial mediation of AOA-IR

To examine whether N_2 production via AOA-IR was mediated by soil microorganisms, we set up a microcosm study in which soils in half the replicates were sterilized to eliminate microbes, and the soils in all replicates were incubated following either +NH_4^+ + $Fe_{(III)}$ or +$Fe_{(III)}$ additions (see Materials and Methods). Under nonsterilized conditions, Fe^{2+} production was elevated in both +NH_4^+ + $Fe_{(III)}$ ($P < 0.01$) and +$Fe_{(III)}$ ($P < 0.05$) compared to the soil control (Fig. 3A), in line with results from experiments 1 and 2 (Fig. 2B and fig. S5). When soils were sterilized, however, neither +NH_4^+ + $Fe_{(III)}$ nor +$Fe_{(III)}$ significantly altered Fe^{2+} production, as compared to the soil control (Fig. 3A), suggesting a key role for soil microbes in coupling IR to AOA.

To determine whether autotrophic or heterotrophic microbes were involved in the AOA-IR process, we designed two SIP microcosm incubations by feeding soil microbial communities with ^{13}C-labeled acetate ($^{13}CH_3{}^{13}COO^-$, SIP 1), a major organic substrate for anaerobes in paddy soils (*24*), and $^{13}CO_2$ (SIP 2), separately (fig. S4C). Upon the measurement of Fe^{2+} production and NH_4^+ consumption (fig. S8, A to D), we verified the occurrence of AOA-IR in two SIP microcosms. We then monitored the changes of headspace $^{13}CO_2$ to determine whether microbes involved in AOA-IR required C from organic (CH_3COO^-) and/or inorganic (CO_2) sources. When soils were amended with $^{13}CH_3{}^{13}COO^-$, $^{13}CO_2$ production remained unchanged in the +NH_4^+, +$Fe_{(III)}$, and +NH_4^+ + $Fe_{(III)}$ treatments (fig. S8E). By contrast, with the addition of $^{13}CO_2$, headspace $^{13}CO_2$ consumption by microbial communities increased with time ($P < 0.05$; fig. S8F), with a higher CO_2 consumption following +NH_4^+ + $Fe_{(III)}$ compared to +NH_4^+, +$Fe_{(III)}$, or the soil control treatment ($P < 0.01$; Fig. 3B). These results imply that microbes involved in AOA-IR were largely autotrophic, rather than heterotrophic.

To identify key microbial community members associated with AOA-IR, we sequenced 16*S* ribosomal RNA (rRNA) gene amplicons for genomic DNA prepared from $^{13}CO_2$-fed soil samples in SIP 2. We separated ^{13}C- from ^{12}C-labeled DNA through ultracentrifugation to identify active autotrophs (see Materials and Methods). A total of 16,366 bacterial and archaeal operational taxonomic units (OTUs) were detected in both ^{12}C- and ^{13}C-labeled microbiota. Microbial communities given +NH_4^+ + $Fe_{(III)}$ were distinctive from those given +NH_4^+ as revealed by the ordination analysis of 16*S* rRNA gene profiles (Fig. 3C) and three nonparametric multivariate statistical tests (table S2). Within both ^{12}C- and ^{13}C-labeled microbiota, the most dominant taxon was the β-Proteobacteria, its relative

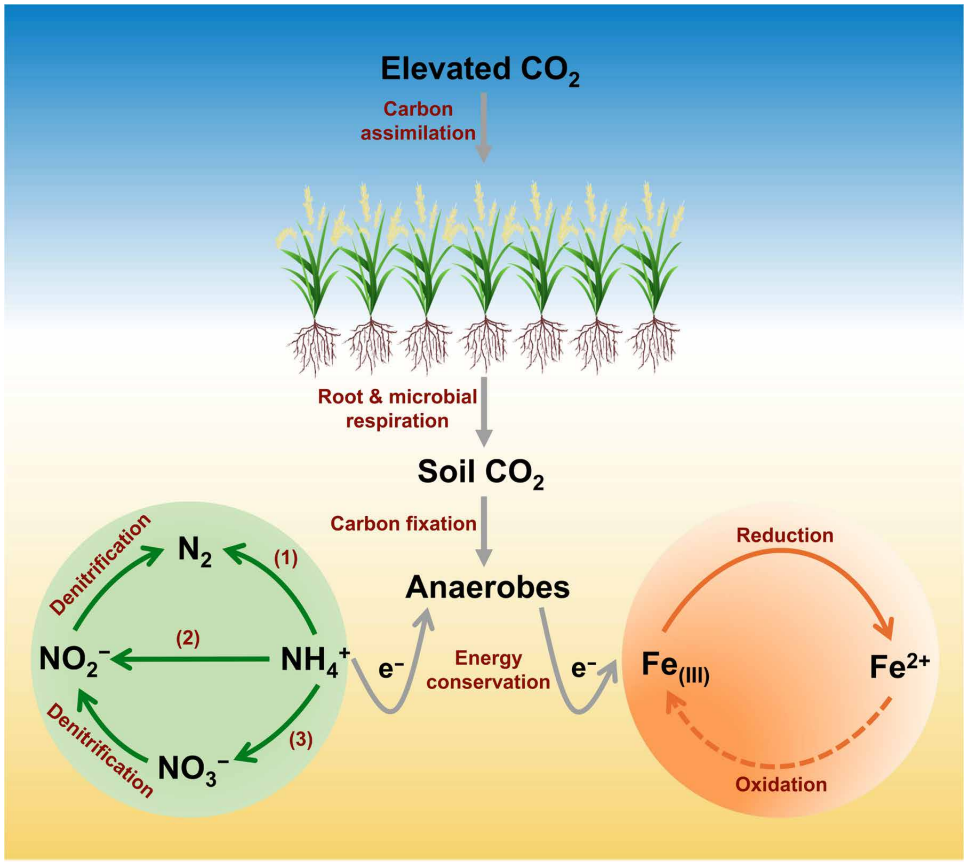

Fig. 4. A conceptual framework of microbial mediation of AOA coupled to IR in a rice ecosystem in response to long-term FACE. CO_2 stimulation of root and microbial activities increases soil CO_2 production, generating a novel niche for certain autotrophic anaerobes that take advantage of CO_2 as their C source; meanwhile, they conserve energy by catalyzing AOA-IR. Left inset: Reactions 1 to 3 of AOA. Right inset: IR. Solid and dashed arrows represent positive and negative CO_2 effects, respectively.

abundance being higher in the $+NH_4^+ + Fe_{(III)}$ than that of the $+NH_4^+$ treatment (fig. S9, A and B). β-Proteobacteria were difficult to culture, but the presence of the most cultures of live β-Proteobacteria in the $+NH_4^+ + Fe_{(III)}$ treatment was confirmed using fluorescence in situ hybridization (FISH) with the BET42a probe (Fig. 3D). Assessment at lower taxonomic levels further points to the prominent role of an unclassified genus within the family Alcaligenaceae, order Burkholderiales (fig. S9, C to F). Within this unclassified genus, a hitherto unclassified OTU accounted for 47% of all detected OTUs at $+NH_4^+ + Fe_{(III)}$ within the ^{13}C-labeled community (Fig. 3E). These results suggest that a previously unknown autotrophic member of β-Proteobacteria is responsible for mediating AOA-IR, although disentangling its complete set of functions will require further metagenomic analyses of enriched cultures.

Ecosystem N balance under eCO_2

This set of investigations reveals a previously unidentified mechanism of CO_2-induced N losses from the rice ecosystems in which rising atmospheric CO_2 may significantly shift the functions of rice paddy soils by favoring an unusual group of autotrophic anaerobes responsible for N_2 volatilization due to ammonium oxidation linked to IR (Fig. 4; also see Discussion III in the Supplementary Materials). Two results emerge. First, CO_2-induced N losses via AOA-IR will cause a decline in soil N retention under eCO_2, as shown by ^{15}N remaining in soil in the in situ field experiment (fig. S10A). The decrease in soil N retention under eCO_2 was coincident with CO_2-induced changes in the size of soil N pool [soil-extractable NH_4^+ (fig. S10B) and soil total N (fig. S10C)] across the experimental years of 2014–2018, likely mitigating the net CO_2 effect on plant N uptake over time (figs. S2B and S10D; also see Discussions I and IV in the Supplementary Materials). Second, our results imply that N_2 production associated with AOA-IR may be substantial (Fig. 2A, fig. S6, and table S3). On the basis of the current projection of NH_4^+-N fertilization in rice ecosystems (*8*–*10*), N losses via AOA-IR from paddy rice systems would be estimated approximately at 4.8 Tg N $year^{-1}$ by the middle of this century (see Materials and Methods), substantially altering terrestrial N cycling under future eCO_2.

The discovery that eCO_2 stimulates anaerobic microbial mediation of AOA-IR might be extrapolated into systems other than rice paddies such as in wetlands and humid tropical forests where anaerobic soil conditions are prevalent (*18*, *19*). Given the widespread observations that eCO_2 enhances anaerobic microbial activity (*1*, *15*, *25*), understanding the CO_2 effect on AOA coupled to reduction of iron and other oxidizers (see Discussion II in the Supplementary Materials) in terrestrial soils should be an active area of research. Although accurate projections of global N losses via AOA-IR from terrestrial ecosystems under future eCO_2 would require further experimental (see Discussion IV in the Supplementary Materials) and

modeling efforts, our results do provide insights into the linkage between terrestrial Fe and N cycles. Last, our findings raise important questions about the efficacy of applying excessive NH_4^+-N fertilizers to sustain crop production under rising atmospheric CO_2 concentrations. We suggest, as have others (*12*, *14*, *26*), that careful matching of crop N demand to N supply in terms of timing and quantity would effectively reduce N fertilizer use and unnecessary loss from agroecosystems.

MATERIALS AND METHODS

Site description and the FACE system

The long-term FACE experiment was initiated to investigate the response of a rice ecosystem to eCO_2 (*15*). The FACE facility was originally established in Wuxi City, Jiangsu Province, China (31°37′N, 120°28′E) in June 2001 (FACE experimental site 1) and then moved to Jiangdu City, Jiangsu Province, China (32°35′N, 119°42′E) in November 2003 (FACE experimental site 2) (*15*). The current work has been mainly conducted at FACE experimental site 2, where annual mean temperature is 14.9°C and annual mean precipitation is 980 mm. Soil bulk density is 1.2 g cm^{-3}. Soil contained 137 g clay kg^{-1} (<0.001 mm), 18 g C kg^{-1}, 1.5 g N kg^{-1}, and 0.6 g P kg^{-1} at the start of the FACE experiment. The soil, a typical rice paddy with the plough pan, is a Mollisol (USA-ST) with a pH of 7.2.

The FACE platform consisted of six octagonal plots, with each of them having a diameter of 12.5-m FACE ring (fig. S1). The six experimental plots represented a randomized complete block design, with each pair of ambient (aCO_2) and elevated CO_2 (ambient + 200 μmol mol^{-1}) plots randomly assigned into three blocks within a 4-ha area. At FACE experimental site 1, CO_2 fumigation was maintained continuously, 24 hour day^{-1} during every rice growing season over the experimental years of 2001–2003 (*15*). At FACE experimental site 2, CO_2 fumigation was initiated in June 2004 and maintained during daylight hours during each rice growing season over the experimental years of 2004–2018 (*16*). Rice seeds were sown under aCO_2 and eCO_2 in every May and then transplanted into their corresponding field plots in each of mid-June. Detailed descriptions of the FACE facility, air CO_2 concentrations, rice planting practices, and fertilization regimes can be found elsewhere (*15*, *16*).

Meta-analysis study

We conducted a meta-analysis study to investigate the influence of eCO_2 on the aboveground biomass, N concentration, and N uptake of rice plants at different levels of N fertilization using previously published data. We searched relevant peer-reviewed articles published before December 2018 using Web of Science (Clarivate Analytics, Boston, MA, USA). Only datasets generated from the current rice-FACE system were selected (Supplementary Datasets). We calculated the effect size of eCO_2 for each individual observation by transforming the response ratio (R) with the natural log: $\ln R = (B_e/B_a)$, where B_e is the mean of plant biomass or N concentration for eCO_2 treatment and B_a is the mean of plant biomass or N concentration for aCO_2 treatment. A mixed model of the meta-analytical software (OpenMEE) was used to calculate the mean effect sizes and 95% confidence intervals (*27*). Data presented in figures were extracted using Engauge Digitizer (http://markummitchell.github.io/engauge-digitizer/).

Experiment 1

We conducted three separate but complementary experiments (experiments 1 to 3) to investigate the influence of eCO_2 on the transformation of ammonium (NH_4^+) in rice paddies under anaerobic conditions at FACE experimental site 2 (fig. S4). Experiment 1 included two parallel laboratory microcosms that were conducted in the years of 2014 and 2015 to examine whether AOA was coupled to IR in rice paddies under eCO_2 (fig. S4A). All soil samples were taken within subplots with the N fertilization rate at 25 g urea-N m^{-2}, corresponding to the moderate fertilization level in East Asia. A soil corer (5 cm in diameter and 10 cm in depth) was used to take soil samples from 0- to 10-cm soil layers of aCO_2 and eCO_2 plots at the heading stage of rice plants in the 11th (2014) and 12th (2015) years of growing seasons, respectively. Soils were sealed in plastic bags, stored immediately in a cooler with dry ice, and transported to the laboratory. In the laboratory, field moist soils of each plot were mixed thoroughly to form one composite sample. Subsamples (~20 g) were then taken immediately, frozen, and stored at −80°C for DNA extraction, and the rest of them were stored at 4°C for laboratory incubation and other analyses.

Fresh soils of each field plot, which were used for incubation, were split into five 20-g dry mass equivalent aliquots and were then mixed with N_2-purged water at a ratio of 1:2 [soil (g):water (ml)]. Each aliquot of soil slurries was placed into a 160-ml serum jar and then preincubated in the dark for 1 week to deplete residual oxygen (O_2), nitrite (NO_2^-), and nitrate (NO_3^-) in an anaerobic glove box (Anaerobic Workstation AW 200SG, Electrotek Scientific Inc., West Yorkshire, UK). The gas composition of the glove-box headspace was 80% dinitrogen gas (N_2), 10% carbon dioxide (CO_2), and 10% hydrogen (H_2). After preincubation, soil slurries were incubated following the addition of ammonium chloride (NH_4Cl, hereafter $+NH_4^+$), amorphous ferric oxyhydroxide [$Fe(OH)_3$, hereafter $+Fe_{(III)}$], NH_4Cl and $Fe_{(III)}$ [hereafter $+NH_4^+ + Fe_{(III)}$], or NH_4Cl and $Fe_{(III)}$ and acetylene (C_2H_2) together [hereafter $+NH_4^+ + Fe_{(III)} + C_2H_2$]. A soil control without any addition of $^{15}NH_4^+$, $Fe_{(III)}$, or C_2H_2 was also accompanied (n = 3 per treatment). Jars treated as blanks were added with sterilized quartz sand (SiO_2) for background gas measurements. Stable isotope ^{15}N-labeled NH_4Cl ($^{15}NH_4Cl$, hereafter $+^{15}NH_4^+$) was used to track the changes of the valance state of NH_4^+. Amorphous ferric oxyhydroxide, a reactive $Fe_{(III)}$ that is rich in paddy soils, was synthesized following the method described previously (*28*). Briefly, 1 M NaOH was added slowly to the solution of 0.2 to 0.4 M $FeCl_3$ with pH controlled at around 6.8. Precipitation was suction-filtered and washed with distilled water to eliminate Cl^- (tested with silver nitrate) and then dried below 60°C in an oven. The addition of C_2H_2 was used to block the conversion of N_2O to N_2 during denitrification (*23*). For both two microcosm incubations, 50 parts per million (ppm) $^{15}NH_4^+$ (deoxygenated) and/or sufficient $Fe_{(III)}$ were added into each of the jars with the corresponding nutrient addition treatment. The amount of added NH_4^+ was chosen according to the moderate level of nitrogen fertilizer application in the field. All ^{15}N-labeled chemicals were purchased as 98% pure (atomic % $^{15}N \geq 98\%$; Sigma-Aldrich). For the C_2H_2 treatment, 1-ml C_2H_2 gas, which accounted for 1% of the volume of jar headspace, was injected into each jar. Every jar was then sealed with a rubber septa and incubated at 30°C in the dark for 1 month in an incubator with the shaking speed at 100 rpm. Except for soil sampling time in the field (sampled in 2014 and 2015, separately), the two parallel microcosms had the same experimental setup (e.g., CO_2 and nutrient addition treatments), incubation procedures, soil solution, and gas sampling.

Experiment 2

Experiment 2 was carried out using an in situ bioreactor in the field in the 13th rice growing season (2016). The anaerobic bioreactor, modified from a dissolved gas sampler (*15*), was constructed using a polyvinyl chloride (PVC) tube (internal diameter = 4.6 cm, height = 20 cm) in which one side was sealed and the other remained open (fig. S4B). One Rhizon soil moisture sampler (RSMS; pore size, 0.1 μm; Eijkelkamp Agrisearch Equipment, Giesbeek, The Netherlands) and one gas sampling port were also embedded on the sealed side of each bioreactor (fig. S4B). To test the feasibility of bioreactors, we did a pre-experiment in the spring 2016 by growing rice plants in the university greenhouse with the addition of either $^{15}NH_4^+$ or $^{15}NH_4^+$ and $Fe_{(III)}$ together. Preliminary results about Fe^{2+} production, plant biomass ^{15}N, and soil remaining ^{15}N showed that the bioreactors were able to maintain a stable anaerobic condition for testing the coupling of AOA and IR reactions in the field.

In the 2016 year rice growing season at FACE experimental site 2, we buried five bioreactors vertically (0- to 10-cm soil layer) into the same subplot of N fertilization as experiment 1 within each of aCO_2 and eCO_2 plots. Within each plot, four bioreactors were added with $^{15}NO_3^-$ (referred to as $+^{15}NO_3^-$), $^{15}NH_4^+$ (referred to as $+^{15}NH_4^+$), $^{15}NH_4^+$ and $Fe_{(III)}$ [referred to as $+^{15}NH_4^+ + Fe_{(III)}$], or $^{15}NH_4^+$ and $^{14}NO_3^-$ (referred to as $+^{15}NH_4^+ + ^{14}NO_3^-$), and the remaining one without any nutrient addition was considered a soil control. A total of 50 ppm ^{15}N tracers and 5 ppm 2-chloro-6-(trichloromethyl) pyridine (daxtron) were injected below the surface of the soil within each bioreactor. The addition of daxtron was used to block the first step of nitrification. At the heading stage, we temporarily drained the field and then flooded it, maintaining ~5-cm water within each bioreactor throughout the experiment. After the first gas sampling, bioreactor headspace was flushed with external air. The height of the water layer within each bioreactor was also recorded for calculating headspace gas volume. Plant and soil samples were collected after the second gas sampling for measurements of plant biomass, soil ^{15}N.

Experiment 3

Two SIP laboratory microcosms were subsequently designed to assess the metabolic type of soil microbes involved in AOA-IR (fig. S4C). Similar to experiment 1, soils used for incubation were taken from both aCO_2 and eCO_2 plots at the heading stage of rice plants in the 14th year growing season (2017). In the first SIP microcosm, we fed soil microbiota with ^{13}C-labeled acetate ($^{13}CH_3{}^{13}COONa$, 98 atomic %; Sigma-Aldrich), a common organic substrate for anaerobes in paddy soils (*28*), to determine whether microbes involved in AOA-IR were heterotrophic. Soils from each plot were divided into four 20-g dry mass equivalent aliquots. A parallel experiment with the addition of $^{12}CH_3{}^{12}COONa$ was also conducted for analytical assurance of gas and chemical measurements. In the second SIP microcosm, we fed soil microbiota with the addition of either $^{13}CO_2$ (5% of headspace, volume/volume) or $^{12}CO_2$ (5% of headspace, volume/volume) to determine whether microbes involved in AOA-IR were autotrophic. The headspace of each jar was flushed every 2 weeks with a $CO_2/H_2/N_2$ (10%/10%/80%) mixed air within the anaerobic glove box, and $^{13}CO_2$ and $^{12}CO_2$ were renewed immediately using degassing method after headspace air exchange. For both two SIP microcosms, we applied four nutrient addition treatments (n = 3) as follows: soil control, $+NH_4^+$, $+Fe_{(III)}$, and $+ NH_4^+ + Fe_{(III)}$. During the course of incubation, 25 ppm NH_4^+ (deoxygenated) and sufficient $Fe_{(III)}$ were supplemented to the corresponding jars every two 2 weeks. Soil sampling, preincubation, and incubation conditions were identical for the two SIP microcosms.

AOA-NR test

AOA-NR is the process of AOA coupled to NR. This is referred to as AOA-NR, also known as "anammox" (*21*, *22*). To determine whether AOA-NR existed in the rice-FACE system, we conduct two AOA-NR tests accompanying with experiments 1 (see the diagram of the experimental scheme in fig. S4A) and 2 (fig. S4B). We set up the laboratory microcosm incubation using soils from aCO_2 and eCO_2 plots at the heading stage of rice plants in the 12th year growing season at FACE experimental site 2. Soils from each field plot were divided into four aliquots: One of them was considered the soil control, and the other three were amended with $^{15}NH_4^+$, $^{15}NO_3^-$, or $^{15}NH_4^+$ and NO_3^- together (mixed with 1:1 mole ratio). Again, jars treated as blanks were added with SiO_2 (n = 3 per treatment) for background gas measurements. Except for the soil control, each incubation jar was added with a total amount of 100 μM N. Incubation of the slurries was stopped after 24 hours by adding 200 μl of a 7 M $ZnCl_2$ solution. Headspace gas samples for $^{29}N_2$ and $^{30}N_2$ determination were taken immediately after the $ZnCl_2$ addition. Gas sampling and storage were identical to those of experiment 1. The potential contributions of AOA-NR and denitrification to N_2 production were calculated on the basis of the analyses of $^{29}N_2$ and $^{30}N_2$ production.

Sterilization test

To test the possibility that soil microbes were involved in the reactions of AOA-IR in rice paddies, we conducted a sterilization laboratory microcosm study using soils only from three aCO_2 plots taken at the heading stage of rice plants in the 12th year growing season at FACE experimental site 2. In the laboratory, soils from each plot were split into two parts: One was autoclaved to eliminate soil biota (referred to as sterilized), and the other was considered a nonsterilization treatment (referred to as nonsterilized). Both sterilized and nonsterilized soils were then divided into three aliquots (20-g equivalent in dry weight): One aliquot was deemed as soil control, and the other two were amended with either $Fe_{(III)}$ or NH_4^+ and $Fe_{(III)}$ together (n = 3). NH_4^+ (50 ppm) (deoxygenated) and sufficient $Fe_{(III)}$ were added into each jar. Soil preparation, preincubation, and incubation conditions were identical to those of experiment 1.

Sampling

Gas sampling

In experiment 1, headspace gas samples for $^{29}N_2$ and $^{30}N_2$ measurements were taken on days 1 and 30 after incubation. After the first gas sampling, headspace gas in each jar was quickly and continuously flushed with a $CO_2/H_2/N_2$ (10%/10%/80%) mixed air within the anaerobic glove box and then maintained at an air pressure of 1 atm. In experiment 2, headspace gas samples for $^{29}N_2$ and $^{30}N_2$ determination were taken on days 1 and 14 after nutrient addition. After the first gas sampling, an equal volume of external air was added back to each of bioreactors to maintain a total pressure of 1 atm. In experiment 3, headspace gas samples for $^{13}CO_2$ measurements were taken in the 4th and 8th week.

At each gas sampling time point, headspace gas was extracted using a gas-tight syringe (Gaoge Industrial and Trading Co. Ltd., Shanghai, China) and then injected into a 12-ml Exetainer evacuated glass vial (Labco Ltd., Wales, UK). For all laboratory incubations, each incubation jar was shaken sufficiently to maintain a balance between headspace and dissolved gases before gas sampling. All laboratory operations were executed in the anaerobic glove box.

Soil solutions

In experiment 1, soil solutions for Fe^{2+} determination were sampled on days 1, 3, 7, 15, and 30 after incubation. In experiment 2, soil solutions were taken through the RSMS on days 1, 7, and 14 after nutrient addition using a 20-ml syringe. Subsamples (500 μl) were immediately acidified by adding 100 μl of 3 M HCl for Fe^{2+} determination. In experiment 3, soil solutions for both Fe^{2+} and NH_4^+ determination were sampled on days 7, 14, 21, and 28 after incubation. In sterilization test, soil solutions for Fe^{2+} determination were sampled on day 14 after incubation.

For all laboratory incubations, 1-ml soil solution was extracted at each sampling time point from a jar using a gas-tight syringe. Subsamples (300 μl) were filtered through a 0.22-μm disposable needle filter and then immediately acidified by adding 100 μl of 3 M HCl for Fe^{2+} determination. The rest of soil solutions were mixed with 2 M KCl for NH_4^+ analysis. All sampling was done in the anaerobic glove box.

Soil DNA extraction

Genomic DNA, for either soil metagenomic sequencing or ^{13}C-DNA separation, was extracted from 5-g aliquots of soil samples using the PowerMax Soil DNA Isolation Kit (MO BIO Laboratories Inc., Carlsbad, CA, USA) according to the manufacturer's instructions. For real-time quantitative polymerase chain reaction (PCR) of the *hzs*A and *amo*A genes, 0.25-g soil samples were used for DNA extraction using the PowerSoil DNA Isolation Kit (MO BIO Laboratories Inc., Carlsbad, CA, USA). Soil DNA quantity and purity were determined using the NanoDrop (ND LITE Spectrophotometer, Thermo Fisher Scientific Inc., Wilmington, DE, USA).

Measurements

Chemical analysis

The concentration of Fe^{2+} in soil solutions was determined using the ferrozine assay described previously (*29*). Briefly, 100-μl subsamples were added to the 1900-μl Pipes-buffered ferrozine solution (pH 7.0, 1 g liter^{-1} ferrozine), and the absorbance was measured at 562 nm on an ultraviolet-visible (UV-Vis) spectrophotometer (Unico Instrument Co. Ltd., Shanghai, China). NH_4^+, NO_2^-, and NO_3^- were extracted from soil slurries with 2 M KCl. NH_4^+ was determined using the indophenol blue assay, and the absorbance was quantified at 625 nm on a UV-Vis spectrophotometer. The concentrations of NO_2^- and NO_3^- were determined using an ion chromatography (DIONEX ICS-3000, Thermo Fisher Scientific, Waltham, MA, USA). N_2H_4 was determined using a spectrophotometric method described previously (*22*). Briefly, 10-ml subsample was reacted with 10 ml of paradimethylaminobenzaldehyde solution and 5 ml of HCl. The absorbance was measured at 458 nm on a UV-Vis spectrophotometer.

Gas and stable isotope analysis

Headspace N_2 was determined using a gas chromatograph (GC 9790II, Fuli Inc., Taizhou, China). The stable isotope ratio of ^{15}N ($^{29}N_2$ and $^{30}N_2$; that is, $^{15}N^{14}N$ and $^{15}N^{15}N$, respectively) in N_2 was determined with an isotope ratio mass spectrometer interfaced with a gas analysis system (MAT 253plus, Thermo Fisher Scientific, Waltham, MA, USA). The production rate of $^{29}N_2$ and $^{30}N_2$ was expressed by

$$^{X}N_2 = \frac{\left[V \times \frac{R(^{X}N_2)}{R(^{28}N_2)}\right]}{V_m} \times M \times M_s^{-1} \times D^{-1}$$

where $^{X}N_2$ is $^{29}N_2$ or $^{30}N_2$, V is the volume of N_2 in the headspace of each jar or bioreactor, R is the mass-to-charge ratio, V_m is the molar volume of a gas that is 22.4 L mol^{-1} at the standard temperature and pressure (STP; 0°C and 101 kPa), M is the molar mass of the gas (g mol^{-1}), M_s is the dry weight of soil samples (grams), and D denotes days after incubation. The net production rate of $^{29}N_2$ and $^{30}N_2$ was calculated using $^{29}N_2$ and $^{30}N_2$ in treatments with the $^{15}NH_4^+$ addition minus those in the soil control treatment.

Gaseous CO_2 in two SIP microcosms of experiment 3 was measured using the gas chromatograph (GC 9790II). The stable isotope ratio of ^{13}C in CO_2 was determined with the Isoprime 100 Isotope Ratio Mass Spectrometer (Agilent Technologies Inc., Santa Clara, CA, USA). The isotope ratio of C was expressed by

$$\delta^{13}C\ (‰) = \left(\frac{R_{sa}}{R_{PDB}} - 1\right) \times 1000$$

where δ is the isotope ratio, R_{sa} is the molar isotope ratio of $^{13}C/^{12}C$, and R_{PDB} is the Pee Dee Belemnite (PDB) standard, which is 0.0112372. The total content of $^{13}CO_2$ production was expressed by

$$^{13}CO_2 = \left(\frac{\delta^{13}C}{1000} + 1\right) \times R_{PDB} \times \frac{V}{V_m}$$

where V is the volume of CO_2 in the jar headspace. The $^{13}CO_2$ consumption was calculated using the amount of added $^{13}CO_2$ before incubation minus the amount of $^{13}CO_2$ remaining in each jar after incubation.

Plant and soil measurements

We determined plant N uptake throughout a whole rice growing season at FACE experimental site 1 in 2003 (*15*). At FACE experimental site 1, three ambient and three elevated CO_2 plots were randomly arranged within a 4-ha area. Each experimental plot was split into two subplots of N supply. The low and high N subplots were applied with 15 g urea-N m^{-2} and 25 g urea-N m^{-2}, respectively. Plant samples were collected on days 30, 51, 78, and 113 after transplanting that corresponded to mid-tillering, jointing, heading, and ripening, respectively. At each sampling time, five individual plants were taken from each plot; carefully divided into leaves, stems, grains, and roots; washed with deionized (DI) water; and dried at 65°C for 2 days to obtain the dry weight measurement. Dried samples were ground, and the N concentrations of each plant part were determined separately using a CHNS/O elemental analyzer (PerkinElmer 2400, Series II, PerkinElmer Inc., Waltham, MA, USA).

Harvested plants from experiment 2 at FACE experimental site 2 were carefully separated into aboveground and belowground parts, washed with DI water, and dried at 65°C for 2 days for the dry weight measurement. Soil samples from experiment 2 for ^{15}N measurement were oven-dried at room temperature and ground using a JXFSTPRP-48 grinding machine (JingXun Industrial Development Co. Ltd., Shanghai, China). The stable N isotope ratio was determined

using the FLASH 2000 Organic Elemental Analyzer (Thermo Fisher Scientific, Waltham, MA, USA). The isotope ratio of N in soils was expressed by

$$\delta^{15}\mathrm{N}\ (‰) = \left(\frac{R_{sa}}{R_{st}} - 1\right) \times 1000$$

where R_{sa} is the isotope ratio of ^{15}N:^{14}N in a soil sample and R_{st} is the isotope ratio of ^{15}N:^{14}N in the standard (that is, atmospheric N_2; R = 0.0036765, $\delta^{15}N$ = 0‰). Soil ^{15}N was calculated from the isotope ratio and total N content of a sample.

Soils, taken from aCO_2 and eCO_2 plots during heading at FACE experimental site 2 from 2014 to 2018, were used for total N and extractable NH_4^+ measurements. Soil samples for total N measurement were air-dried and ground using a JXFSTPRP-48 grinding machine (JingXun Industrial Development Co. Ltd., Shanghai, China). Soil total N was determined using the Kjeldahl method. Soil NH_4^+ was extracted with 2 M KCl using fresh soil samples, and the NH_4^+ concentrations were determined using the indophenol blue assay.

Reverse transcription quantitative PCR

Real-time quantitative PCR of *hzs*A and *amo*A genes was performed to determine changes of the abundance of anammox bacteria (*22*) and ammonia-oxidizing archaea and bacteria (*30*), respectively. Amplifications and detections were performed on the CFX Connect Real-Time System (Bio-Rad Laboratories Inc., Hercules, CA, USA). The PCR conditions and primer pairs of anammox bacteria and ammonia-oxidizing archaea and bacteria are shown in table S4. Meanwhile, the abundance of the whole soil bacteria was quantified with the primer pair EUb338 of the 16*S* rRNA gene (*31*). The 20-μl reaction mixture contained 10 μl of SYBR Premix Ex Taq (Bio-Rad Laboratories Inc., Hercules, CA, USA), 1 μl of each primer (anammox bacteria, ammonia-oxidizing archaea and bacteria, or the whole soil bacteria), and 4 μl of template DNA. Three technical replicates were performed for each quantitative PCR assay. A known copy number of plasmid DNA was serially diluted 10-fold to generate the external standard curve in the real-time PCR. Melting curves were used to check the specificity of amplification. The correlation coefficient (R) of amplification efficiencies was used when R^2 was above 0.98.

^{13}C-DNA separation

We extracted genomic DNA from the second SIP microcosm ($+^{13}CO_2$) of experiment 3 and separated ^{13}C-labeled DNA from unlabeled community (^{12}C-DNA) using the gradient fractionation method (*32*, *33*). Briefly, 3 μg of genomic DNA was mixed with gradient buffer (GB; 0.1 M tris, 0.1 M KCl, and 1 mM EDTA) to a final volume of 1 ml. The GB/DNA mixture was then combined with the CsCl solution (1.870 g ml^{-1}) to a final volume of 6.00 ml and then loaded in a polyallomer bell-top Quick-Seal centrifuge tube (Beckman Coulter Inc., Fullerton, CA, USA). Centrifuge tubes were sealed, put into the Vti-65 rotor, and then spun at 50,800 rpm and 20°C for 60 hours with vacuum in a Himac CP 80β ultracentrifuge (Hitachi Koko Co. Ltd., Tokyo, Japan). A fraction recovery system (Beckman Coulter Inc., Fullerton, CA) in connection with a syringe pump (model R-100E, Razel, Georgia, VT) was used to retrieve DNA gradients. The buoyant density of gradient fractions was determined using a refractometer (AR200, Reichert, Depew, NY, USA). DNA from gradient fractions was precipitated with isopropanol at 25°C for 2 hours.

16S rRNA gene sequencing

16*S* rRNA genes of each SIP sample were amplified using the primer set 515F/806R (table S4) (*34*). PCR was performed using a PCR cycler (Eppendorf AG, Hamburg, GER). Each biological sample was amplified with three tagged primers as three technical replicates. Each 100-μl PCR mixture contained 3.5 μl of template DNA, 1 μl of each primer, 4 μl of 2.5 mM deoxynucleotide triphosphate (dNTP), 5 μl of 10× PCR buffer, and 0.5 μl of Taq DNA polymerase. The thermocycling conditions are shown in table S4. Agarose (1.0%) gel electrophoresis was performed to purify PCR products of each technical sample. All amplified PCR products were then recycled using the BioSpin Gel Extraction Kit (Bioer Technology Co. Ltd., Hangzhou, China) and quantified using a Nanodrop LITE spectrophotometer. Samples were mixed in an equimolar concentration and sequenced on an Illumina HiSeq 2500 platform (Illumina Inc., San Diego, CA, USA).

Microbial community profiling

Acquired raw sequencing data were processed following the procedure described earlier (*33*). Read trimming and downstream analyses were performed using QIIME (*35*). Briefly, we trimmed reads at an accuracy threshold of 0.5% per base error probability and then removed bar codes and primers. Reads were removed if they did not match exactly to a bar code and primer. The OTUs were defined at 97% identity threshold after removing low-quality or ambiguous reads. The resulting OTU tables were used for further phylogenetic and statistical analyses using the R software (version 3.1, The R Foundation for Statistical Computing, 2013).

Fluorescence in situ hybridization

All bacteria and β-Proteobacteria were detected using FISH with the EUB338 and BET 42a primers (table S4) (*31*). Soil samples from experiment 3 were fixed using the 4% paraformaldehyde solution, and then lysozyme solution was used for prokaryotic cell wall permeabilization. The BET 42a probe (table S4) labeled by the dye Cy3 on the 5′ end was used to complete the hybridization step. Last, the picture is captured with an Eclipse NI-U fluorescence microscope (Nikon Co. Ltd., Tokyo, Japan).

Metagenomic sequencing and data analysis

Genomic DNA of six samples from aCO_2 and eCO_2 plots was sequenced using the Illumina HiSeq 2500 platform. A total of 30,060,977 to 44,558,285 pairs of reads of 100–base pair length were obtained for each of samples. Reads were subject to quality control using the btrim program (*36*) with an average quality score of 20 and window size at 3. Remained reads were directly searched against the m5nr database (*37*) using the DIAMOND program. The best hit for each read was extracted for functional profiling. Metagenomic functional profiles were extracted on the basis of the Kyoto Encyclopedia of Genes and Genomes (KEGG) ontology information (*38*). Random subsampling was carried out on the basis of the smallest value of the total number of reads mapped to KEGG ontologies. The relative abundance of each gene was determined by comparing the number of hits and dividing by the total number of hits to the KEGG database. The response ratio of functional genes was calculated as follows: (the abundance of genes at eCO_2 – the abundance of genes at aCO_2)/the abundance of genes in aCO_2.

Thermodynamic favorability of AOA-IR reactions

Thermodynamic favorability of AOA-IR reactions was represented by Gibbs free energy. The changes of Gibbs free energies of AOA-IR reactions were calculated using related equations described earlier (*19*). Briefly, the generalized reaction was expressed as

$$aA + bB \rightarrow cC + dD$$

The Gibbs free energy of a balanced reaction was calculated from the following

$$\Delta G^{\circ\prime} = \Delta G^{\circ} + RT \ln \frac{\{C\}^c \{D\}^d}{\{A\}^a \{B\}^b}$$

where ΔG° was calculated by

$$\Delta G^{\circ} = c\Delta G^{\circ}_{fC} + d\Delta G^{\circ}_{fD} - a\Delta G^{\circ}_{fA} - b\Delta G^{\circ}_{fB}$$

where a, b, c, and d are the number of moles; ΔG°_{fC} and ΔG°_{fD} denote the free energy of formation for the products (C and D); ΔG°_{fA} and ΔG°_{fB} represent the free energy of formation for the reactants (A and B); R is the gas constant (which is 0.008314 kJ mol^{-1} K), and T is the absolute temperature in Kelvin (which is 297.15 K). The chemical activity values used in this study are at a pH of 6.5, which is within the normal range of pH values of most paddy soils under flooded conditions (*20*). Notice that thermodynamic favorability of three reactions would be larger at much lower pH (values of $\Delta G^{\circ\prime}$ were not provided). We used free energies of the products and reactants described earlier (*39*): NH_4^+ = −79.37 kJ mol^{-1}; $Fe_{(III)}$ = −699 kJ mol^{-1}; Fe^{2+} = −78.87 kJ mol^{-1}; N_2 = 0 kJ mol^{-1}; H^+ = 0 kJ mol^{-1}; NO_2^- = −37.2 kJ mol^{-1}; NO_3^- = −111.3 kJ mol^{-1}; H_2O = −237.18 kJ mol^{-1}.

Stoichiometry of AOA-IR reactions

In experiment 1, we used a linear model to estimate the Fe^{2+}:N_2 ratio of AOA-IR reactions. The presence of C_2H_2 did not affect Fe^{2+} production in soil; we thus assumed that intercepts were identical for the $+NH_4^+ + Fe_{(III)}$ and $+NH_4^+ + Fe_{(III)} + C_2H_2$ treatment. We then used a dump variable t to represent the two treatments [t = 0 for the $+NH_4^+ + Fe_{(III)}$ treatment; t = 1 for the $+NH_4^+ + Fe_{(III)} + C_2H_2$ treatment]. The equation of the linear model can be written as

$$c(Fe^{2+}) = c(N_2) + c(N_2) \times t$$

where $c(N_2) \times t$ denotes the interaction between $c(N_2)$ and t.

Ecosystem N loss via AOA-IR under eCO_2

We estimated the relative contribution of three AOA-IR reactions [AOA-IR directly to N_2 (reaction 1) or AOA-IR to NO_2^-/NO_3^- (reactions 2 and 3)] to the total N_2 production by comparing the difference between the rates of N_2 ($^{30}N_2 + {}^{29}N_2$) production with and without the C_2H_2 addition. The presence of C_2H_2 allowed inhibiting the reduction of N_2O to N_2, thus blocking N_2 production from reactions 2 and 3.

We combined N_2 ($^{29}N + {}^{30}N$) production data from the field and the stoichiometry of AOA-IR reactions estimated from experiment 1 to estimate ecosystem N losses through AOA-IR under eCO_2. The rate of ^{15}N-NH_4^+ oxidation in the field was calculated from the difference of N_2 ($^{29}N + {}^{30}N$) production between the $+^{15}NH_4^+$ and soil control treatment. Because the potential of denitrification was very high in both microcosm and field experiments, we assumed that any NO_x^- generated from reactions 2 and 3 would be completely converted to N_2 through denitrification. The ratio of the lost N via AOA-IR to the total applied N was expressed as

$$\text{N loss (\%)} = \frac{\left[V \times \frac{R(^X N_2)}{R(^{28}N_2)}\right]}{\frac{V_m}{(1 - Rs) \times T}} \times M \times 100\%$$

where $^XN_2$ is $^{29}N_2$ or $^{30}N_2$, V is the volume of N_2 in the headspace of each jar or bioreactor, R is the mass-to-charge ratio, V_m is the molar volume of a gas [which is 22.4 L mol^{-1} at the STP (0°C and 101 kPa, respectively)], M is the molar mass of the gas (g mol^{-1}), R_s is the percentage of ^{15}N recovered in soil, and T is the total amount of applied ^{15}N-NH_4^+ fertilizer. The total amount of NH_4^+-N fertilizer application in global rice ecosystems in 2050 was estimated using the approach in the literature (*8*, *9*). Global N losses via AOA-IR from rice ecosystems by the middle of this century were calculated using the percentage of N loss estimated in the current study multiplying the total amount of world NH_4^+-N fertilizer application.

Data analyses

To analyze the effect of eCO_2 on N losses following the addition of NH_4^+ alone, we used datasets of ^{15}N-N_2 (the total amount of $^{29}N_2$ and $^{30}N_2$) production on day 1 from experiments 1 and 2, and NH_4^+ consumption during the first week from experiment 3, as presented in Fig. 1. Datasets of $^{29}N_2$ and $^{30}N_2$ production on day 30 from experiment 1 and on day 14 from experiment 2 presented in fig. S6 were used to analyze the coupling of AOA and IR. Datasets of ^{15}N-N_2 and Fe^{2+} production over the whole incubation from experiment 1 presented in Fig. 2 were used to calculate the stoichiometry of AOA-IR reactions.

Data from experiments 1 to 3 were subjected to analysis of variance (ANOVA) using the linear mixed-effects (LME) model (*6*). The LME model used to analyze the datasets from experiment 1 ($^{30}N_2$ and $^{29}N_2$ production on days 1 and 30 or Fe^{2+} production on day 30), experiment 2 ($^{30}N_2$ and $^{29}N_2$ production on days 1 and 14 or Fe^{2+} production on day 14), and AOA-NR test ($^{30}N_2$ and $^{29}N_2$ production on day 1) is written as

$$y_{ijk} = a + b_i + c_j + n_k + (c \times n)_{jk} + b_{ij} + e_{ijk}$$

where y_{ijk} is the total production of N_2 and Fe^{2+}, a is the intercept (fixed effects), b_i is the block (fixed effects), c_j is the CO_2 treatment (fixed effects), n_k is the nutrient addition treatment ($+^{15}NH_4^+$, $+Fe_{(III)}$, $+^{15}NH_4^+ + Fe_{(III)}$, or $+^{15}NH_4^+ + Fe_{(III)} + C_2H_2$; fixed effects), $(c \times n)_{jk}$ is the CO_2 and nutrient addition interaction (fixed effects), b_{ij} is the CO_2 within block (random effects), and e_{ijk} is the random experimental error.

Datasets from experiments 1 and 2 (Fe^{2+} production over the course of incubation) and 3 (Fe^{2+}, NH_4^+, and $^{13}CO_2$ production or consumption over the course of incubation) were analyzed using the LME model as follows

$$y_{ijkl} = a + b_i + c_j + n_k + (c \times n)_{jk} + t_l + (c \times t)_{jl} + (n \times t)_{kl} + (c \times n \times t)_{jkl} + b_{ij} + e_{ijk}$$

where y_{ijkl} is Fe^{2+} production and other variables; a is the intercept (fixed effects); b_i is the block (fixed effects); c_j is the CO_2 treatment (fixed effects); n_k is the nutrient addition treatment [$+Fe_{(III)}$ or $+^{15}NH_4^+ + Fe_{(III)}$; fixed effects]; $(c \times n)_{jk}$ is the CO_2 and nutrient addition (fixed effects); t_l is the time effect (fixed effects); $(c \times t)_{jl}$ is the CO_2 and time interaction (fixed effects); $(n \times t)_{kl}$ is the interaction of nutrient addition and time (fixed effects); $(c \times n \times t)_{jkl}$ is the

interaction of CO_2, nutrient addition, and time (fixed effects); b_{ij} is the CO_2 within block (random effects); and e_{ijk} is the random experimental error.

The data with time series measurements for soil N (NH_4^+ and total N) at FACE experimental site 2 were analyzed using a repeated-measures mixed model (*6*)

$$y_{ijkl} = a + b_i + c_j + p_{ij} + t_k + (c \times t)_{jk} + e_{ijk}$$

where y_{ijkl} is soil NH_4^+ or soil total N, a is the intercept (fixed effects), b_i is the block (fixed effects), c_j is the CO_2 treatment (fixed effects), p_{ij} is the plot effects within blocks (random effects), t_k is the time effect (fixed effects), $(c \times t)_{jk}$ is the CO_2 and time interaction (fixed effects), and e_{ijk} is the random experimental error.

Significance test for paired comparisons ($^{30}N_2$, $^{29}N_2$, and Fe^{2+} production in aCO_2 or eCO_2 soils under a given nutrient addition treatment in experiments 1 and 2; $^{13}CO_2$ production and consumption under different nutrient addition treatments in experiment 3) was performed using the Tukey's HSD (honestly significant difference) functions. The two-way ANOVA with the general linear model was used to analyze datasets from sterilization test.

We used nonmetric multidimensional analysis (NMDS) to assess the similarity of different microbial communities based on 16*S* rRNA sequencing datasets from experiment 3. Results from principal components analysis (PCA) and detrended correspondence analysis were very similar to those generated from NMDS. Three different but complementary nonparametric multivariate statistical analysis methods were used to test statistical differences of microbial communities between the ^{12}C-DNA and ^{13}C-DNA communities or the $+NH_4^+$ and $+NH_4^+ + Fe_{(III)}$ treatments. The three methods are permutational multivariate ANOVA using distance matrices (Adonis), analysis of similarities (ANOSIM), and multiresponse permutation procedure (MRPP). All 16*S* rRNA sequencing data were analyzed on the basis of biological replicates. *P* values of the relative abundance of taxa (16*S* rRNA sequencing datasets) and the signal intensity of functional genes (metagenomic sequencing datasets) were calculated using paired two-tailed *t* tests. PCA, Adonis, ANOSIM, and MRPP were analyzed using the "vegan" package (*40*).

All statistical analyses were performed using the R software (version 3.1, The R Foundation for Statistical Computing, 2013). Significant differences were accepted at a $P < 0.05$.

SUPPLEMENTARY MATERIALS

Supplementary material for this article is available at http://advances.sciencemag.org/cgi/content/full/6/42/eabb7433/DC1

View/request a protocol for this paper from *Bio-protocol*.

REFERENCES AND NOTES

1. S. Hu, M. K. Firestone, F. S. Chapin III, Soil microbial feedbacks to atmospheric CO_2 enrichment. *Trends Ecol. Evol.* **14**, 433–437 (1999).
2. B. A. Hungate, J. S. Dukes, M. R. Shaw, Y. Q. Luo, C. B. Field, Nitrogen and climate change. *Science* **302**, 1512–1513 (2003).
3. Y. Luo, B. Su, W. S. Currie, J. S. Dukes, A. C. Finzi, U. Hartwig, B. Hungate, R. E. McMurtrie, R. Oren, W. J. Parton, D. E. Pataki, M. R. Shaw, D. R. Zak, C. B. Field, Progressive nitrogen limitation of ecosystem responses to rising atmospheric carbon dioxide. *Bioscience* **54**, 731–739 (2004).
4. P. B. Reich, B. A. Hungate, Y. Luo, Carbon-nitrogen interactions in terrestrial ecosystems in response to rising atmospheric carbon dioxide. *Annu. Rev. Ecol. Evol. Syst.* **37**, 611–636 (2006).
5. A. J. Bloom, M. Burger, J. S. Rubio-Asensio, A. B. Cousins, Carbon dioxide enrichment inhibits nitrate assimilation in wheat and arabidopsis. *Science* **328**, 899–903 (2010).
6. L. Cheng, F. L. Booker, C. Tu, K. O. Burkey, L. Zhou, H. D. Shew, T. W. Rufty, S. Hu, Arbuscular mycorrhizal fungi increase organic carbon decomposition under elevated CO_2. *Science* **337**, 1084–1087 (2012).
7. P. B. Reich, S. E. Hobbie, Decade-long soil nitrogen constraint on the CO_2 fertilization of plant biomass. *Nat. Clim. Chang.* **3**, 278–282 (2013).
8. P. E. Fixen, F. B. West, Nitrogen fertilizers: Meeting contemporary challenges. *Ambio* **31**, 169–176 (2002).
9. J. N. Galloway, F. J. Dentener, D. G. Capone, E. W. Boyer, R. W. Howarth, S. P. Seitzinger, G. P. Asner, C. C. Cleveland, P. A. Green, E. A. Holland, D. M. Karl, A. F. Michaels, J. H. Porter, A. R. Townsend, C. J. Vorosmarty, Nitrogen cycles: Past, present, and future. *Biogeochemistry* **70**, 153–226 (2004).
10. D. E. Canfield, A. N. Glazer, P. G. Falkowski, The evolution and future of Earth's nitrogen cycle. *Science* **330**, 192–196 (2010).
11. B. L. Bodirsky, A. Popp, H. Lotze-Campen, J. P. Dietrich, S. Rolinski, I. Weindl, C. Schmitz, C. Mueller, M. Bonsch, F. Humpenoeder, A. Biewald, M. Stevanovic, Reactive nitrogen requirements to feed the world in 2050 and potential to mitigate nitrogen pollution. *Nat. Commun.* **5**, 3858 (2014).
12. C. Yu, X. Huang, H. Chen, H. C. J. Godfray, J. S. Wright, J. W. Hall, P. Gong, S. Ni, S. Qiao, G. Huang, Y. Xiao, J. Zhang, Z. Feng, X. Ju, P. Ciais, N. C. Stenseth, D. O. Hessen, Z. Sun, L. Yu, W. Cai, H. Fu, X. Huang, C. Zhang, H. Liu, J. Taylor, Managing nitrogen to restore water quality in China. *Nature* **567**, 516–520 (2019).
13. Z. Zhu, Q. Wen, J. Freney, Nitrogen in soils of China, in *Springer Series in Developments in Plant and Soil Sciences* (Springer, 1997), vol. 74.
14. X. Ju, G. Xing, X. Chen, S. Zhang, L. Zhang, X. Liu, Z. Cui, B. Yin, P. Christie, Z. Zhu, F. Zhang, Reducing environmental risk by improving N management in intensive Chinese agricultural systems. *Proc. Natl. Acad. Sci. U.S.A.* **106**, 3041–3046 (2009).
15. L. Cheng, J. Zhu, G. Chen, X. Zheng, N. H. Oh, T. W. Rufty, D. deB Richter, S. Hu, Atmospheric CO_2 enrichment facilitates cation release from soil. *Ecol. Lett.* **13**, 284–291 (2010).
16. C. Zhu, K. Kobayashi, I. Loladze, J. Zhu, Q. Jiang, X. Xu, G. Liu, S. Seneweera, K. L. Ebi, A. Drewnowski, N. K. Fukagawa, L. H. Ziska, Carbon dioxide (CO_2) levels this century will alter the protein, micronutrients, and vitamin content of rice grains with potential health consequences for the poorest rice-dependent countries. *Sci. Adv.* **4**, eaaq1012 (2018).
17. G. Chen, Z. Yong, Y. Liao, D. Zhang, Y. Chen, H. Zhang, J. Chen, J. Zhu, D. Xu, Photosynthetic acclimation in rice leaves to free-air CO_2 enrichment related to both ribulose-1,5-bisphosphate carboxylation limitation and ribulose-1,5-bisphosphate regeneration limitation. *Plant Cell Physiol.* **46**, 1036–1045 (2005).
18. J. C. Clement, J. Shrestha, J. G. Ehrenfeld, P. R. Jaffe, Ammonium oxidation coupled to dissimilatory reduction of iron under anaerobic conditions in wetland soils. *Soil Biol. Biochem.* **37**, 2323–2328 (2005).
19. W. H. Yang, K. A. Weber, W. L. Silver, Nitrogen loss from soil through anaerobic ammonium oxidation coupled to iron reduction. *Nat. Geosci.* **5**, 538–541 (2012).
20. F. N. Ponnamperuma, in *Soils and Rice* (IRRI, 1978), pp. 420–441.
21. M. Strous, J. A. Fuerst, E. H. M. Kramer, S. Logemann, G. Muyzer, K. T. van de Pas-Schoonen, R. Webb, J. G. Kuenen, M. S. M. Jetten, Missing lithotroph identified as new planctomycete. *Nature* **400**, 446–449 (1999).
22. B. Kartal, W. J. Maalcke, N. M. de Almeida, I. Cirpus, J. Gloerich, W. Geerts, H. J. M. O. den Camp, H. R. Harhangi, E. M. Janssen-Megens, K.-J. Francoijs, H. G. Stunnenberg, J. T. Keltjens, M. S. M. Jetten, M. Strous, Molecular mechanism of anaerobic ammonium oxidation. *Nature* **479**, 127-U159 (2011).
23. T. Yoshinari, R. Hynes, R. Knowles, Acetylene inhibition of nitrous oxide reduction and measurement of denitrification and nitrogen fixation in soil. *Soil Biol. Biochem.* **9**, 177–183 (1977).
24. T. Yoshida, in *Soil Biochemistry*, E. A. Paul, A. D. McLaren, Eds. (Marcel Dekker Inc., 1975), vol. 3.
25. J. W. H. Dacey, B. G. Drake, M. J. Klug, Stimulation of methane emission by carbon dioxide enrichment of marsh vegetation. *Nature* **370**, 47–49 (1994).
26. A. Williams, A. S. Davis, P. M. Ewing, A. S. Grandy, D. A. Kane, R. T. Koide, D. A. Mortensen, R. G. Smith, S. S. Snapp, K. A. Spokas, A. C. Yannarell, N. R. Jordan, Precision control of soil nitrogen cycling via soil functional zone management. *Agric. Ecosyst. Environ.* **231**, 291–295 (2016).
27. B. C. Wallace, M. J. Lajeunesse, G. Dietz, I. J. Dahabreh, T. A. Trikalinos, C. H. Schmid, J. Gurevitch, OpenMEE: Intuitive, open-source software for meta-analysis in ecology and evolutionary biology. *Methods Ecol. Evol.* **8**, 941–947 (2017).
28. D. R. Lovley, E. J. P. Phillips, Organic matter mineralization with reduction of ferric iron in anaerobic sediments. *Appl. Environ. Microbiol.* **51**, 683–689 (1986).
29. J. Sorensen, Reduction of ferric iron in anaerobic, marine sediment and interaction with reduction of nitrate and sulfate. *Appl. Environ. Microbiol.* **43**, 319–324 (1982).
30. J. H. Rotthauwe, K. P. Witzel, W. Liesack, The ammonia monooxygenase structural gene amoA as a functional marker: Molecular fine-scale analysis of natural ammonia-oxidizing populations. *Appl. Environ. Microbiol.* **63**, 4704–4712 (1997).

31. R. I. Amann, B. J. Binder, R. J. Olson, S. W. Chisholm, R. Devereux, D. A. Stahl, Combination of 16S rRNA-targeted oligonucleotide probes with flow cytometry for analyzing mixed microbial populations. *Appl. Environ. Microbiol.* **56**, 1919–1925 (1990).
32. J. D. Neufeld, J. Vohra, M. G. Dumont, T. Lueders, M. Manefield, M. W. Friedrich, J. C. Murrell, DNA stable-isotope probing. *Nat. Protoc.* **2**, 860–866 (2007).
33. L. Cheng, N. Zhang, M. Yuan, J. Xiao, Y. Qin, Y. Deng, Q. Tu, K. Xue, J. D. Van Nostrand, L. Wu, Z. He, X. Zhou, M. B. Leigh, K. T. Konstantinidis, E. A. G. Schuur, Y. Luo, J. M. Tiedje, J. Zhou, Warming enhances old organic carbon decomposition through altering functional microbial communities. *ISME J.* **11**, 1825–1835 (2017).
34. W. Walters, E. R. Hyde, D. Berg-Lyons, G. Ackermann, G. Humphrey, A. Parada, J. A. Gilbert, J. K. Jansson, J. G. Caporaso, J. A. Fuhrman, A. Apprill, R. Knight, Improved bacterial 16S rRNA gene (V4 and V4-5) and fungal internal transcribed spacer marker gene primers for microbial community surveys. *mSystems* **1**, e00009-15 (2016).
35. J. G. Caporaso, J. Kuczynski, J. Stombaugh, K. Bittinger, F. D. Bushman, E. K. Costello, N. Fierer, A. G. Pena, J. K. Goodrich, J. I. Gordon, G. A. Huttley, S. T. Kelley, D. Knights, J. E. Koenig, R. E. Ley, C. A. Lozupone, D. McDonald, B. D. Muegge, M. Pirrung, J. Reeder, J. R. Sevinsky, P. J. Tumbaugh, W. A. Walters, J. Widmann, T. Yatsunenko, J. Zaneveld, R. Knight, QIIME allows analysis of high-throughput community sequencing data. *Nat. Methods* **7**, 335–336 (2010).
36. Y. Kong, Btrim: A fast, lightweight adapter and quality trimming program for next-generation sequencing technologies. *Genomics* **98**, 152–153 (2011).
37. A. Wilke, T. Harrison, J. Wilkening, D. Field, E. M. Glass, N. Kyrpides, K. Mavrommatis, F. Meyer, The M5nr: A novel non-redundant database containing protein sequences and annotations from multiple sources and associated tools. *BMC Bioinformatics* **13**, 141 (2012).
38. M. Kanehisa, S. Goto, KEGG: Kyoto encyclopedia of genes and genomes. *Nucleic Acids Res.* **28**, 27–30 (2000).
39. W. Stumm, J. Morgan, Aquatic chemistry: Chemical equilibria and rates in natural waters. *Environ. Sci. Technol.* **11**, (1996).
40. P. Dixon, VEGAN, a package of R functions for community ecology. *J. Veg. Sci.* **14**, 927–930 (2003).
41. P. M. Vitousek, R. W. Howarth, Nitrogen limitation on land and in the sea: How can it occur? *Biogeochemistry* **13**, 87–115 (1991).
42. R. R. Northup, Z. Yu, R. A. Dahlgren, K. A. Vogt, Polyphenol control of nitrogen release from pine litter. *Nature* **377**, 227–229 (1995).
43. G. A. Kowalchuk, J. R. Stephen, Ammonia-oxidizing bacteria: A model for molecular microbial ecology. *Annu. Rev. Microbiol.* **55**, 485–529 (2001).
44. J. N. Galloway, A. R. Townsend, J. W. Erisman, M. Bekunda, Z. Cai, J. R. Freney, L. A. Martinelli, S. P. Seitzinger, M. A. Sutton, Transformation of the nitrogen cycle: Recent trends, questions, and potential solutions. *Science* **320**, 889–892 (2008).
45. I. Koegel-Knabner, W. Amelung, Z. Cao, S. Fiedler, P. Frenzel, R. Jahn, K. Kalbitz, A. Koelbl, M. Schloter, Biogeochemistry of paddy soils. *Geoderma* **157**, 1–14 (2010).
46. I. Arth, P. Frenzel, Nitrification and denitrification in the rhizosphere of rice: The detection of processes by a new multi-channel electrode. *Biol. Fertil. Soils* **31**, 427–435 (2000).
47. T. D. Colmer, Long-distance transport of gases in plants: A perspective on internal aeration and radial oxygen loss from roots. *Plant Cell Environ.* **26**, 17–36 (2003).
48. S. Liu, P. Han, L. Hink, J. I. Prosser, M. Wagner, N. Bruggemann, Abiotic conversion of extracellular NH_2OH contributes to N_2O emission during ammonia oxidation. *Environ. Sci. Technol.* **51**, 13122–13132 (2017).
49. G. Zhu, S. Wang, Y. Wang, C. Wang, N. Risgaard-Petersen, M. S. M. Jetten, C. Yin, Anaerobic ammonia oxidation in a fertilized paddy soil. *ISME J.* **5**, 1905–1912 (2011).
50. D. R. Lovley, Dissimilatory Fe(III) and Mn(IV) reduction. *Microbiol. Rev.* **55**, 259–287 (1991).
51. J. E. Dore, R. Lukas, D. W. Sadler, M. J. Church, D. M. Karl, Physical and biogeochemical modulation of ocean acidification in the central North Pacific. *Proc. Natl. Acad. Sci. U.S.A.* **106**, 12235–12240 (2009).
52. K. E. Fabricius, C. Langdon, S. Uthicke, C. Humphrey, S. Noonan, G. De'ath, R. Okazaki, N. Muehllehner, M. S. Glas, J. M. Lough, Losers and winners in coral reefs acclimatized to elevated carbon dioxide concentrations. *Nat. Clim. Chang.* **1**, 165–169 (2011).
53. J. A. Andrews, W. H. Schlesinger, Soil CO_2 dynamics, acidification, and chemical weathering in a temperate forest with experimental CO_2 enrichment. *Glob. Biogeochem. Cycles* **15**, 149–162 (2001).
54. B. A. Hungate, E. A. Holland, R. B. Jackson, F. S. Chapin, H. A. Mooney, C. B. Field, The fate of carbon in grasslands under carbon dioxide enrichment. *Nature* **388**, 576–579 (1997).
55. D. R. Zak, K. S. Pregitzer, J. S. King, W. E. Holmes, Elevated atmospheric CO_2, fine roots and the response of soil microorganisms: A review and hypothesis. *New Phytol.* **147**, 201–222 (2000).
56. K. J. van Groenigen, X. Qi, C. W. Osenberg, Y. Luo, B. A. Hungate, Faster decomposition under increased atmospheric CO_2 limits soil carbon storage. *Science* **344**, 508–509 (2014).
57. D. A. Wardle, R. D. Bardgett, J. N. Klironomos, H. Setala, W. H. van der Putten, D. H. Wall, Ecological linkages between aboveground and belowground biota. *Science* **304**, 1629–1633 (2004).
58. L. Cheng, thesis, University of Chinese Academy of Sciences (2004).
59. N. H. Oh, D. D. Richter Jr., Soil acidification induced by elevated atmospheric CO_2. *Glob. Chang. Biol.* **10**, 1936–1946 (2004).
60. E. L. Williams, L. M. Walter, T. C. W. Ku, G. W. Kling, D. R. Zak, Effects of CO_2 and nutrient availability on mineral weathering in controlled tree growth experiments. *Glob. Biogeochem. Cycles* **17**, 1041 (2003).
61. H. Ma, H. Zhu, G. Liu, Z. Xie, Y. Wang, L. Yang, Q. Zeng, Availability of soil nitrogen and phosphorus in a typical rice-wheat rotation system under elevated atmospheric CO_2. *Field Crop Res.* **100**, 44–51 (2007).
62. B. Xie, Z. Zhou, B. Mei, X. Zheng, H. Dong, R. Wang, S. Han, F. Cui, Y. Wang, J. Zhu, Influences of free-air CO_2 enrichment (FACE), nitrogen fertilizer and crop residue incorporation on CH_4 emissions from irrigated rice fields. *Nutr. Cycl. Agroecosyst.* **93**, 373–385 (2012).
63. W. Du, J. L. Gardea-Torresdey, Y. Xie, Y. Yin, J. Zhu, X. Zhang, R. Ji, K. Gu, J. R. Peralta-Videa, H. Guo, Elevated CO_2 levels modify TiO_2 nanoparticle effects on rice and soil microbial communities. *Sci. Total Environ.* **578**, 408–416 (2017).
64. C. Zhu, X. Xu, D. Wang, J. Zhu, G. Liu, An indica rice genotype showed a similar yield enhancement to that of hybrid rice under free air carbon dioxide enrichment. *Sci. Rep.* **5**, 12719 (2015).
65. S. Lai, S. Zhuang, Y. Wu, Y. Wang, J. Zhu, L. Yang, Y. Wang, Impact of elevated atmospheric CO_2 concentration and temperature on growth and development of super rice. *Chin. J. Ecol.* **34**, 1253–1262 (2015).
66. C. Li, J. Zhu, L. Sha, J. Zhang, Q. Zeng, G. Liu, Rice (*Oryza sativa L.*) growth and nitrogen distribution under elevated CO_2 concentration and air temperature. *Ecol. Res.* **32**, 405–411 (2017).
67. C. Chen, Q. Jiang, L. H. Ziska, J. Zhu, G. Liu, J. Zhang, K. Ni, S. Seneweera, C. Zhu, Seed vigor of contrasting rice cultivars in response to elevated carbon dioxide. *Field Crop Res.* **178**, 63–68 (2015).
68. C. Zhu, Q. Zeng, A. McMichael, K. L. Ebi, K. Ni, A. S. Khan, J. Zhu, G. Liu, X. Zhang, L. Cheng, L. H. Ziska, Historical and experimental evidence for enhanced concentration of artemesinin, a global anti-malarial treatment, with recent and projected increases in atmospheric carbon dioxide. *Clim. Chang.* **132**, 295–306 (2015).
69. Q. Zeng, B. Liu, B. Gilna, Y. Zhang, C. Zhu, H. Ma, J. Pang, G. Chen, J. Zhu, Elevated CO_2 effects on nutrient competition between a C_3 crop (*Oryza sativa L.*) and a C_4 weed (*Echinochloa crusgalli L.*). *Nutr. Cycl. Agroecosyst.* **89**, 93–104 (2011).
70. X. Chen, J. Zhu, L. Wang, D. Jiang, J. Yan, X. Xu, Q. Zeng, Competition between rice and barnyardgrass at different generations under free-air CO_2 enrichment. *Chin. J. Rice Sci.* **24**, 99–102 (2010).
71. C. Zhu, J. Zhu, J. Cao, Q. Jiang, G. Liu, L. H. Ziska, Biochemical and molecular characteristics of leaf photosynthesis and relative seed yield of two contrasting rice cultivars in response to elevated CO_2. *J. Exp. Bot.* **65**, 6049–6056 (2014).
72. G. Zhang, H. Sakai, T. Tokida, Y. Usui, C. Zhu, H. Nakamura, M. Yoshimoto, M. Fukuoka, K. Kobayashi, T. Hasegawa, The effects of free-air CO_2 enrichment (FACE) on carbon and nitrogen accumulation in grains of rice (*Oryza sativa L.*). *J. Exp. Bot.* **64**, 3179–3188 (2013).
73. L. Yang, H. Huang, H. Yang, G. Dong, H. Liu, G. Liu, J. Zhu, Y. Wang, Seasonal changes in the effects of free-air CO_2 enrichment (FACE) on nitrogen (N) uptake and utilization of rice at three levels of N fertilization. *Field Crop Res.* **100**, 189–199 (2007).
74. C. Zhu, Q. Zeng, H. Yu, S. Liu, G. Dong, J. Zhu, Effect of elevated CO_2 on the growth and macronutrient (N, P and K) uptake of annual wormwood (*Artemisia annua L.*). *Pedosphere* **26**, 235–242 (2016).
75. L. Wang, J. Zhu, C. Zhu, J. Cao, M. Wang, Q. Zeng, Z. Xie, G. Liu, Relationship between decrease in nitrogen content and activities of key enzymes related to nitrogen metabolism in rice leaves under elevated CO_2 concentration. *Chin. J. Rice Sci.* **22**, 499–506 (2008).
76. H. Liu, L. Yang, J. Huang, G. Dong, J. Zhu, G. Liu, Y. Wang, Effect of free-air CO_2 enrichment (FACE) on nitrogen uptake and utilization of three-line indica hybrid rice cultivar Shanyou 63. *J. Agro Environ. Sci.* **27**, 1015–1021 (2008).
77. L. Yang, H. Liu, Y. Wang, J. Zhu, J. Huang, G. Liu, G. Dong, Y. Wang, Impact of elevated CO_2 concentration on inter-subspecific hybrid rice cultivar Liangyoupeijiu under fully open-air field conditions. *Field Crop Res.* **112**, 7–15 (2009).
78. H. Ma, J. Zhu, J. Xie, Q. Zeng, G. Liu, Effects of CO_2 enrichment on the allocation of biomass and C, N uptake in rice organs. *Chin. J. Eco-Agric.* **13**, 38–41 (2005).
79. W. Wang, C. Cai, S. K. Lam, G. Liu, J. Zhu, Elevated CO_2 cannot compensate for japonica grain yield losses under increasing air temperature because of the decrease in spikelet density. *Eur. J. Agron.* **99**, 21–29 (2018).

Acknowledgments: We thank W. H. Yang and C. Yu for their comments on the early version of this paper. We also thank technical assistance from Y. Han, G. Liu, and G. Zhu for maintaining FACE facilities, D. Jia for sequencing, and X. Sun and X. Zhang for stable isotope analyses. **Funding:** This work was supported by grants from the National Natural Science Foundation of China (NSFC# 31670501, 91951107, 31370487, and 31422010), the Zhejiang Provincial NSFC (LR14C030001), and the Fundamental Research Funds for the Central Universities. **Author**

contributions: L.C. and C.X. conceived and designed the study with help from J.Z., S.H., R.T.K., and M.K.F. J.Z. maintained FACE facility 1. J.Z. and Chunwu Zhu maintained FACE facility 2 and provided help for sampling. C.X. mainly performed the research with help from K.Z., W.Z., Chen Zhu, N.Z., F.Y., and S.L. C.X., K.Z., J.X., Chen Zhu, W.Z., N.Z., F.Y., S.L., Q.T., S.H., R.T.K., M.K.F., and L.C. analyzed the data. C.X. and L.C. wrote the first draft with contributions from K.Z., W.Z., J.X., Q.T., X.C., J.Z., S.H., R.T.K., and M.K.F. **Competing interests:** The authors declare that they have no competing interests. **Data and materials availability:** All data needed to evaluate the conclusions in the paper are present in the paper and/or the Supplementary Materials. Additional data related to this paper may be requested from the authors. Correspondence and requests for materials should be addressed to L.C. (lcheng@zju.edu.cn). Tables S1 to S4 and datasets S1 to S3 included in the meta-analysis and 16*S* rRNA sequencing datasets are deposited in the Dryad Repository (doi:10.5061/dryad.612jm6415) https://datadryad.org/stash/share/UfoMLqMgGXdX_rkjVbfHsXebQQs6hob4evDodKmMrFw.

Submitted 16 March 2020
Accepted 28 August 2020
Published 16 October 2020
10.1126/sciadv.abb7433

Citation: C. Xu, K. Zhang, W. Zhu, J. Xiao, C. Zhu, N. Zhang, F. Yu, S. Li, C. Zhu, Q. Tu, X. Chen, J. Zhu, S. Hu, R. T. Koide, M. K. Firestone, L. Cheng, Large losses of ammonium-nitrogen from a rice ecosystem under elevated CO_2. *Sci. Adv.* **6**, eabb7433 (2020).